Review

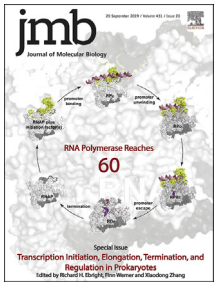

A Single-Molecule View of Archaeal Transcription

Kevin Kramm [1], Ulrike Endesfelder [2] and Dina Grohmann [1]

*1 - **Institute of Biochemistry,** Genetics and Microbiology, University of Regensburg, Universitätsstraße 31, 93053 Regensburg, Germany*
*2 - **Department of Systems and Synthetic Microbiology,** Max Planck Institute for Terrestrial Microbiology and LOEWE Center for Synthetic Microbiology (SYNMIKRO), Karl-von-Frisch-Str. 16, 35043 Marburg, Germany*

***Correspondence to Dina Grohmann:** Institute of Biochemistry, Genetics and Microbiology, University of Regensburg, Universitätsstraße 31, 93053 Regensburg, Germany. dina.grohmann@ur.de.*
https://doi.org/10.1016/j.jmb.2019.06.009

Abstract

The discovery of the archaeal domain of life is tightly connected to an in-depth analysis of the prokaryotic RNA world. In addition to Carl Woese's approach to use the sequence of the 16S rRNA gene as phylogenetic marker, the finding of Karl Stetter and Wolfram Zillig that archaeal RNA polymerases (RNAPs) were nothing like the bacterial RNAP but are more complex enzymes that resemble the eukaryotic RNAPII was one of the key findings supporting the idea that archaea constitute the third major branch on the tree of life. This breakthrough in transcriptional research 40 years ago paved the way for in-depth studies of the transcription machinery in archaea. However, although the archaeal RNAP and the basal transcription factors that fine-tune the activity of the RNAP during the transcription cycle are long known, we still lack information concerning the architecture and dynamics of archaeal transcription complexes. In this context, single-molecule measurements were instrumental as they provided crucial insights into the process of transcription initiation, the architecture of the initiation complex and the dynamics of mobile elements of the RNAP. In this review, we discuss single-molecule approaches suitable to examine molecular mechanisms of transcription and highlight findings that shaped our understanding of the archaeal transcription apparatus. We furthermore explore the possibilities and challenges of next-generation single-molecule techniques, for example, super-resolution microscopy and single-molecule tracking, and ask whether these approaches will ultimately allow us to investigate archaeal transcription *in vivo*.

Introduction

Studies by Stetter and Zillig in the late 1980s showed that the subunit composition of archaeal RNA polymerases (RNAPs) differs significantly from the bacterial subunit composition and is more akin to its eukaryotic RNAP II counterpart [1]. Not only the number of subunits but also the amino acid sequence of the archaeal RNAP shows clear homology to the respective RNAP II subunits (Table 1). RNAPs from all three domains of life feature a conserved three-dimensional architecture (for a comprehensive review of the conserved structure–function relationship of multi-subunit RNAPs, see, e.g., Refs. [1–3]). Bacterial RNAPs consist of subunits α, β, β′ and ω and homologous subunits (Rpo/Rpb 1, 2, 3, 6 and 11) are found in Archaea and Eukaryotes. The largest subunits (β, β′ and Rpo/Rpb1,2) form a "crab-claw"-like structure and contact the downstream DNA. Moreover, the catalytic site of multi-subunit RNAPs is found at the interface of the largest subunits. Many structural elements are conserved among multi-subunit RNAPs, for example, the bridge helix that connects the large subunits and the conformational flexible clamp domain that is formed by the largest subunit. A

Table I. Evolutionary conservation of RNAP subunits in the three domains of life. Summary of bacterial, archaeal and eukaryotic RNAP I, II and III subunits. Rows represent homologous subunits. The molecular functions are indicated in the right column. *Rpo1 and/or Rpo2 are split into two separate subunits in some archaeal species. **Only present in some species of the archaeal TACK (*T*haumarchaeota, *A*igaarchaeota, *C*renarchaeota and *K*orarchaeota) and ASGARD superphyla.

	Bacteria	Archaea	Eukaryotes			
			RNAP II	RNAP III	RNAP I	
Core subunits	β'	Rpo1'/1'' *	Rpb1	C160	A190	Catalysis
	β	Rpo2'/2'' *	Rpb2	C128	A135	
	α_I	Rpo3	Rpb3	AC40		Assembly platform
	α_{II}	Rpo11	Rpb11	AC19		
	ω	Rpo6	Rpb6	Rpb6	Rpb6	RNAP assembly and stability
Eukaryote/archaea specific subunits		Rpo5	Rpb5	Rpb5	Rpb5	dsDNA binding
		Rpo8 **	Rpb8	Rpb8	Rpb8	RNA binding
		Rpo10	Rpb10	Rpb10	Rpb10	Assembly platform
		Rpo12	Rpb12	Rpb12	Rpb12	
		Rpo4	Rpb4	C17	A14	RNA binding (processivity/termination)
		Rpo7	Rpb7	C25	A43	
Polymerase specific subunits		Rpo13 **				dsDNA binding
			Rpb9	C11	A12	Transcript cleavage
				C37	A34.5	Elongation speed, accuracy, processivity and termination
				C53	A49	
				C82		PIC formation DNA melting
				C34		
				C31		

prominent feature that distinguishes archaeal–eukaryotic RNAPs from bacterial RNAPs is the so-called "stalk" domain formed by subunits 4 and 7.

RNAPs and transcriptional complexes were consistently interrogated at the single-molecule level ever since single-molecule measurements could be carried out under physiological conditions [4–9]. However, Archaea arrived late in the single-molecule field as archaeal transcription systems that can be manipulated and equipped with fluorescent probes are sparse. The fully recombinant transcription system from the hyperthermophilic archaeon *Methanocaldococcus jannaschii*, however, provided the possibility to site-specifically engineer fluorescent probes rendering the system suitable for smFRET measurements [10]. In the absence of structural information about the archaeal initiation (IC) or elongation complex (EC), these single-molecule data provided crucial information about the architecture and dynamics of transcription complexes over the last 10 years.

Here, we will discuss the mechanistic and structural insights into the archaeal transcription machinery gained by single-molecule measurements. In addition, we will briefly discuss the opportunities that the single-molecule localization microscopy (SMLM) and single-molecule tracking (SMT) revolution offer to expand our understanding of transcription in the cellular context and will highlight the challenges to implement SMLM and SMT imaging in the archaeal world.

Mechanisms and Dynamics of Transcription Initiation

TBP-induced promoter DNA bending

smFRET is an excellent tool to observe dynamic biomolecular processes in a time-resolved manner. As many transcription factors not only bind but also bend DNA in a sequence-specific fashion, smFRET can be exploited to monitor the DNA bending process [11,12]. In the context of transcription, the DNA is bent at the promoter region during transcription initiation. Archaeal promoter architecture is highly conserved [3,13] and cis-regulatory elements

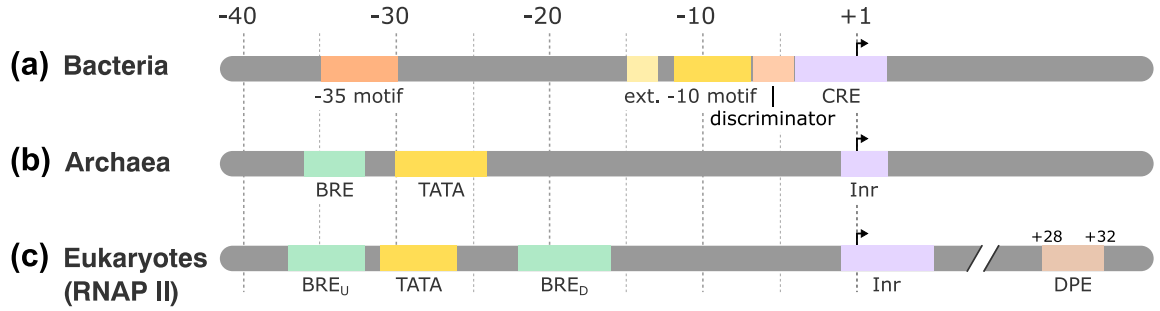

Fig. 1. Common promoter architecture in bacteria, archaea and eukaryotes. (a) Schematic representation of a bacterial (σ70 dependent) promoter: the −35, extended −10, −10 motif and discriminator element are recognized by the σ4, σ3, σ2 and σ1.2 domains of the σ70 initiation factor. The RNAP contacts the core recognition element (CRE) surrounding the transcription start site (+1). (b) Schematic representation of an archaeal promoter. The TATA-box and BRE are recognized by TBP and TFB. (c) Schematic representation of a eukaryotic (human) RNAP II promoter: The TATA-box and upstream/downstream (u/d) BRE are recognized by TBP and the transcription factor IIB (TFIIB). Archaeal and eukaryotic promoters feature the initiator (Inr) element surrounding the transcription start site. RNAPII promoters contain in addition a downstream promoter element (DPE). The sequence position relative to the transcription start site is indicated by dashed lines. Adapted from Ref. [3].

like the TATA-box and the B recognition element (BRE) upstream of the transcription start site are shared between Archaea and Eukaryotes (Fig. 1). During transcription initiation, the highly conserved eukaryotic–archaeal transcription initiation factor TATA-binding protein (TBP) recognizes the TATA-box element in the promoter DNA and bends the DNA upon binding [14,15]. In Archaea, transcription initiation factor TFB (transcription factor B) binds additionally to the BRE upstream of the TATA-box

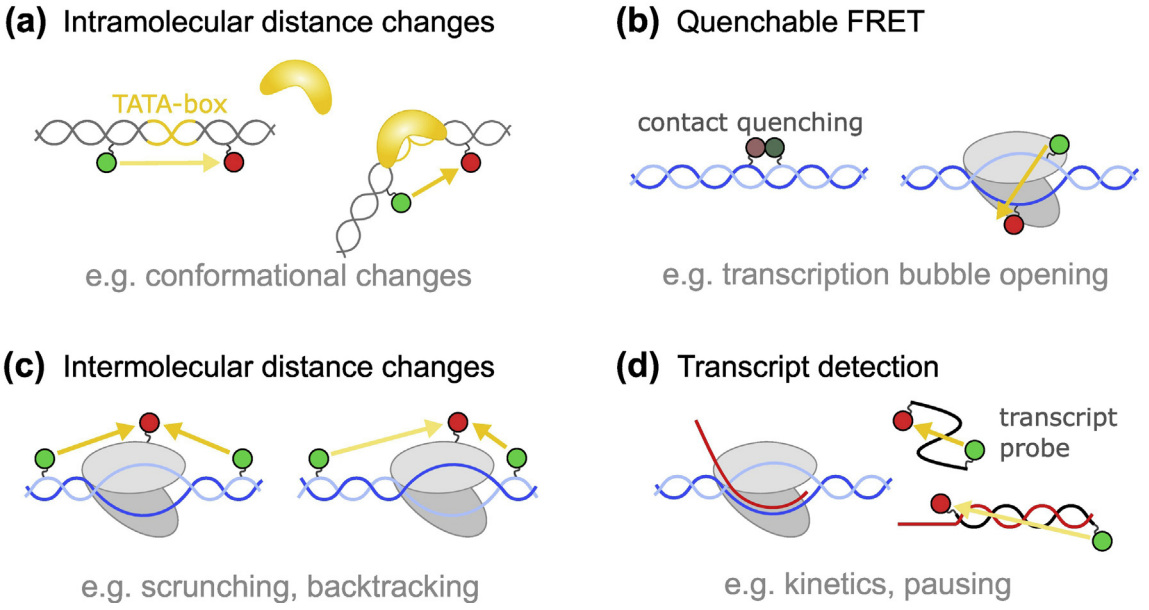

Fig. 2. Single-molecule FRET assays developed to study the molecular mechanisms of transcription. Förster resonance energy transfer (indicated by yellow arrows) between a donor (green) and acceptor (red) fluorophore can be used to probe the structural dynamics of transcription complexes. (a) Intramolecular distance changes of the promoter DNA can be monitored with FRET and can reveal the conformational change of the DNA upon binding of TBP to the TATA-box of the promoter. (b) Contact quenching of fluorescent dyes (qFRET) can be exploited to track small conformational changes or subpopulation with low occurrence rate. The opening of the transcription bubble was monitor via qFRET. (c) Distance changes of proteins in relation to other component of higher order complexes give information on directional movement, for example, scrunching of downstream DNA by bacterial RNAP. (d) The detection of RNA transcripts at the single-molecule level via a complementary donor/acceptor-labeled probe reveals transcription kinetics at biologically relevant protein/NTP concentrations.

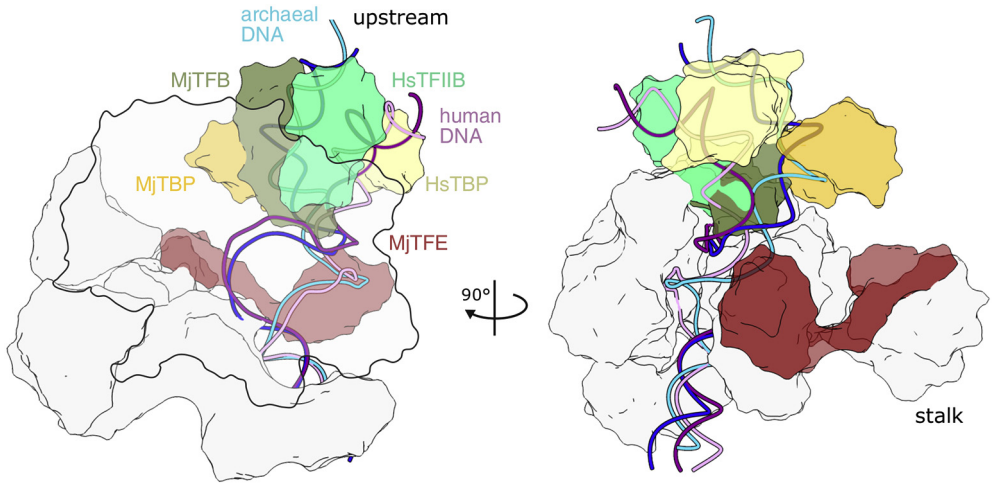

Fig. 3. Structural organization of the archaeal open PIC. Structural superposition of the promoter DNA (archaeal DNA in blue/cyan, eukaryotic DNA in purple/pink) and the initiation factors TFB/TF(II)B (color-coded in green), TFE (color-coded in brown) and TBP (color-coded in yellow) from the archaeon *M. jannaschii* (model from Ref. [40]) and *Homo sapiens* (PDB: 5IYB [41]).

[16–18]. Association of TFB stabilizes the TBP–DNA complex and allows the recruitment of the RNAP via TFB's C-terminal domain [19,20], thereby placing the RNAP in the correct orientation on the promoter. In order to follow the bending of DNA by TBP, a donor–acceptor FRET pair has to be incorporated into the promoter DNA flanking the TATA-box at a distance that results in a low efficiency energy transfer signal (low FRET). DNA binding and bending by TBP reduces the distance between donor and acceptor, which results in a higher FRET efficiency (high FRET) signal (Fig. 2a). Hence, FRET provides a very sensitive readout to determine the degree of DNA-bending and to follow

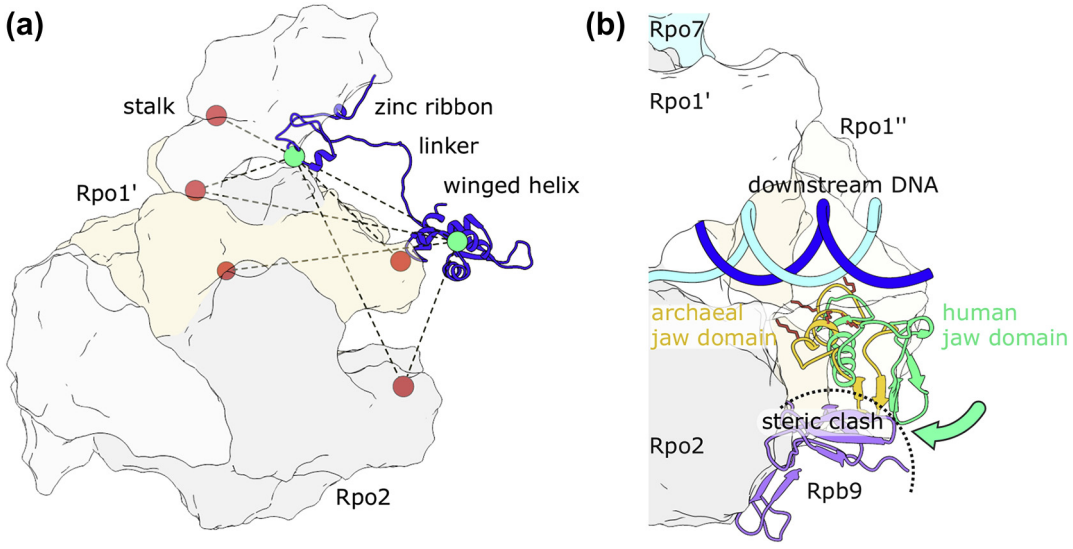

Fig. 4. The NPS utilizes FRET-derived distances as basis for structural modeling. (a) The position of transcription factor E (TFE; blue) on the surface of the RNAP can be calculated from a network of distance constraints. The distances between known position on the polymerase (red) and two labeled position in the zinc ribbon and winged helix domain of TFE (green) were determined with single-molecule FRET experiments. (b) Structural superposition of the archaeal (yellow) and human (green) RNAP jaw domain. In archaea, the jaw domain is positioned closer to the downstream DNA, which allows stabilization via a patch of positively charged amino acids (red). A similar positioning is prevented in the human enzyme due to sterical clashes with the Rpb9 subunit (purple), which is not present in most archaea.

the TBP association and dissociation process in real-time [21–24]. This approach was exploited to gain a mechanistic understanding of the archaeal transcription initiation mechanism [21,25]. Comparing the initiation process of the (hyper-)thermophillic archaeal organisms *M. jannaschii* (optimal growth temperature 85 °C) and *Sulfolobus acidocaldarius* (optimal growth temperature 75 °C), a striking difference was detected: *M. jannaschii* TBP alone is sufficient to bend DNA, while promoter DNA bending in *S. acidocaldarius* strictly requires TBP and TFB. The DNA–TBP complex lifetime in *M. jannaschii* is very short (0.2 s). Interestingly, addition of TFB does not increase the complex lifetime. The DNA–TBP–TFB complex of *S. acidocaldarius* is an order of magnitude more stable with a lifetime of 2.5 s. In both cases, the lifetime of the bent state is unaffected by temperature showing similar lifetimes at 22 °C and at 60 °C [21]. Overall, these experiments revealed that TBP-induced bending of the promoter is more dynamic in Archaea as compared to the eukaryotic RNAP II system from yeast. Here, DNA–TBP complexes are stable for minutes to hours and DNA bending follows a linear three state transition [21,24,26–28]. The first transition from the unbent to intermediate bent state most likely corresponds to the first set of phenylalanines inserting between the bases in the TATA-box sequence. The fully bent state has a similar 80° bending angle [29] as observed for the archaeal TBP–DNA complexes. An intermediate state was not observed in the archaeal systems. Interestingly, a single-step bending mechanism was also observed for the interaction of eukaryotic TBP with the U6 snRNA promoter that is transcribed by the eukaryotic RNAP III [30].

The advent of new nanotechnological devices based on the DNA origami technique extended the technical possibilities to ascertain how molecular forces affect the binding of transcription factors to DNA [31] or the forces between nucleosomes [32]. The recently developed nanoscopic DNA origami force clamp makes use of the smFRET assay that monitors TBP-induced bending as described above but exploits the entropic spring behavior of single-stranded DNA to exert a force in the 2- to 20-pN range on the DNA. *M. jannaschii* TBP-induced bending of the promoter is highly force-dependent and gradually decreases as the force on the promoter DNA increases. Interestingly, the bending angle is independent of the force applied as all experiments showed the same high FRET population of the bent state [31].

These results suggest that an additional layer of transcriptional regulation might exist in Archaea as some archaeal organisms encode histone proteins that can form extended chromatin-like structures termed "hyper-nucleosomes" [33–35]. In this scenario, histone proteins block access of TBP to the DNA and the strain exerted on the DNA in the context of (hyper-)nucleosomes might affect TBP-binding efficiencies.

Promoter DNA opening and initial transcription

The multistep process of transcription initiation was first studied in detail in bacterial transcription systems and provided extraordinary insights into the intricate mechanisms governing the initiation phase of bacterial transcription [36]. As smFRET is one of the few tools to study DNA melting in real-time, DNA opening during transcription initiation could be studied exploiting the fact that some fluorophores (e.g., Cy3B and Atto647N) are quenched when located in extreme proximity (< 2 nm/~3–4 nt distance) [37] (Fig. 2b). Further experiments aimed to dissect promoter opening in more detail [38]. In one study, donor and acceptor fluorophores were positioned in the DNA upstream and downstream of the transcription bubble, respectively, to observe promoter opening upon association of the RNAP holoenzyme with the DNA. In this study, significant conformational heterogeneity among the ICs was detected and three DNA conformations were identified. However, an assignment of these conformations to structural states on the pathway to the fully opened transcriptional bubble was only possible for the high FRET state, which most likely corresponds to the open IC. However, dynamic switching between these states could be observed and the transcription bubble exhibits global conformational dynamics between the closed and fully opened complex at the 100-ms timescale [38]. The conformational fluctuations of the bubble only occur after complex formation with the RNAP holoenzyme. Based on these data, it seems plausible that DNA unwinding only occurs after the double-stranded promoter DNA has been loaded and secured into the DNA binding channel of the RNAP (the so-called "bend-load-open model" for open complex formation [39]) [38].

In the bacterial system, however, no TBP-like factor is encoded and DNA bending is invoked by the σ factor–RNAP complex only. Nevertheless, DNA bending is a universal mechanism that stimulates DNA opening by destabilization of the DNA duplex upon bending. Opening of the DNA in the archaeal IC is furthermore supported by torsional strain and two initiation factors not present in the bacterial system, the transcription initiation factors B and E (TFB and TFE). A structural model of the archaeal open IC (see the Structural Model of the Archaeal Pre-initiation complex section) revealed that the TBP–TFB module is located closer to the surface of the RNAP as compared to the highly homologs RNAP II IC [40] (Fig. 3). The overall closer proximity of TBP and TFB to the RNAP surface and stabilization of downstream DNA by the jaw domain (a part of the RNAP at the tip of one of the "crab claws" that contacts the downstream DNA) likely induces

torsional strain in the DNA, which enables DNA melting without the need for a DNA helicase (Fig. 4b). Further experiments showed that TFE stimulates promoter-directed transcription by stabilization of the IC [19,42–46]. The structural model of the archaeal IC showed that the winged helix domain of TFE is located in close proximity to the upstream edge of the transcription bubble, thereby stabilizing the open IC via its interaction with the non-template strand (NTS) (Fig. 4a). The contribution of TFE to the stabilization of the open complex could be further analyzed by smFRET experiments that monitored the conformational state of the RNAP clamp domain (see The Conformational Landscape of the RNAP Clamp section). The mobile RNAP clamp exists in an equilibrium between an open and closed stated in the IC corresponding to an opened and closed state of the DNA, respectively. In the presence of TFE, this equilibrium is shifted toward the open clamp and the opened DNA [47]. The TFB linker domain lines the inner side of the clamp and was found to interact with the NTS thereby preventing re-annealing of the opened DNA [40,48]. smFRET measurements showed that the TFB linker also adopts two conformational states in the IC mirroring the open and closed state of the clamp [49]. This observation led to the conclusion that the TFB linker moves concomitantly with the clamp upon addition of TFE. Hence, TFE not only exerts its stabilizing effect by the stabilization of the transcription bubble via direct interactions with the DNA but by a structural rearrangement of mobile elements of the RNAP and TFB, which ultimately ensures stable open complex formation.

After recruitment to the promoter and melting of the DNA duplex, the RNAP often engages in repetitive synthesis of short (3–9 nt) RNAs—a phenomena coined abortive initiation [50–52]. Single-molecule experiments revealed that during bacterial abortive initiation, the downstream DNA is reeled into the RNAP in a mechanism called "scrunching" [53,54] that results in stressed RNAP–DNA complexes. The stressed intermediate can release the stored kinetic energy either by releasing the RNAP or by breaking the stabilizing interactions with initiation factors and proceed into productive elongation [53]. Similarly, the stable complex formed by TBP, TFB, TFE, RNAP and the DNA during the initiation phase of archaeal transcription needs to be disrupted upon progression to the elongation phase. However, there are no data available so far that reveal whether scrunching occurs in the archaeal system and whether this provides energy to destabilize the IC. Despite the possibility that DNA scrunching plays a role, the topological transition of TFB domains (e.g., the TFB reader) are also decisive steps in the transition from the initiation to elongation phase in Archaea [49]. The clash of the B-reader helix with the advancing RNA is thought to initiate the release of the TFB helix at position +9/+10 [48]. Further RNA synthesis results in the full release of TFB at position +15 as the RNA finally clashes with the TFB zinc ribbon domain [49]. In addition, the displacement of TFE by the elongation factor Spt4/5 supports the transition into the elongation phase of transcription [13,42,55]. SmFRET experiments that mapped the interaction sites of the TFE winged helix and zinc ribbon domain laid also the basis for the postulation of the so-called "factor exchange mechanism." In this model, the TFE winged helix interacts with the RNAP clamp coiled coil domain as does Spt4/5 [40,42,56]. Hence, binding to the RNAP is mutually exclusive and a displacement of TFE from this binding site is required to allow association of Spt4/5. Global Chip-Seq studies supported this view showing that Spt4/5 association occurs only in the gene body and not at the promoter [13].

Other phenomena described for bacterial RNAPs based on single-molecule data are pausing and backtracking during the initiation process [57–59]. Duchi *et al*. [59] demonstrated that initial transcription is interrupted by a long pause (termed "initiation pause") on the path to productive elongation. This pause occurs after transcription of the first six nucleotides. At this stage, the 5′-end is colliding with the sigma 3.2 region that accommodates the RNA exit channel. Transition into elongation requires the displacement of the sigma 3.2 domain and the "initiation pause" state might reflect a situation in which the RNA contacts sigma 3.2. This might induce a structural rearrangement of sigma 3.2. Another study made use of a fluorescence-based single-molecule assay that is based on the detection of the released RNA transcript via a doubly labeled detection DNA oligonucleotide complementary to the RNA transcript (Fig. 2d [57]). The detection oligonucleotide exhibits a high FRET due to the random folding of the DNA in the absence of the complementary RNA. Progression of the RNAP into the elongation phase leads to the release of the nascent transcript [in this case 20 nt (poly A) in length]. Hybridization of the RNA transcript to the detection oligonucleotide leads to a low FRET signal as the donor and acceptor dye are getting separated by the ordered RNA/DNA duplex. The respective change from a high to low FRET signal allows the measurement of the kinetics of run-off transcript production. Recording the transcription kinetics from ICs that differ in the length of the initially transcribed RNA (either 2, 4, 6 or 7 nt), it could be demonstrated that further elongation of the initial transcribed sequence is delayed if the initial transcribed sequence is longer than 2 nt and shorter than 11 nt. Additional magnetic tweezer experiments demonstrated that this delay is due to a long-lived backtracked state [57]. This backtracked state, however, is an off-pathway state that does not directly lead to productive transcription elongation

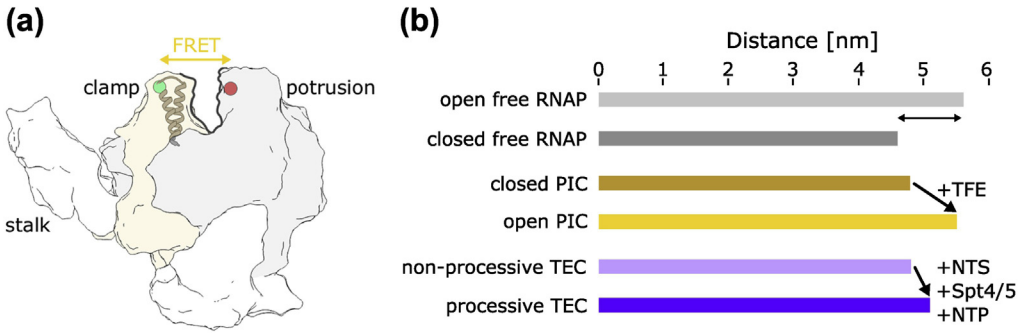

Fig. 5. Conformational landscape of the RNAP clamp. (a) The distance between a donor (green) and acceptor (red) fluorophore engineered into the clamp and protrusion domain of the RNAP was measured using single-molecule FRET experiments. (b) The conformational state of the mobile clamp can be influenced by a variety of factors in the different stages of the transcription cycle. The RNAP fluctuates between an open and closed conformation. In the PIC, binding of transcription factor E (TFE) promotes DNA melting and transition from a closed to open clamp. The transcription EC (TEC) exists in two states distinguishable by the conformational state of the clamp that either adopts a closed or open form that correspond a processive or non-processive complex, respectively. The processive form is strongly favored in the presence of the NTS, nucleotide triphosphates (NTPs) and the elongation factor Spt4/5.

but requires cleavage of the backtracked RNA to resume transcription, or alternatively, the RNA is released from the IC (abortive transcription). Further insights into transcriptional pausing and backtracking were gained by a study by Dulin *et al*. [58]. This study showed that a significant fraction of ICs do not enter the processive transcription pathway after the initiation pause at nucleotide six but enter a repetitive DNA scrunching/unscrunching cycle that keeps the bacterial RNAP in an inactive state (e.g., at limiting NTP concentrations in the cell). The authors suggest that this inactive RNAP either can return to the productive pathway (once normal cellular NTP concentrations are restored) or enters the backtracked state that leads to abortive transcription.

These measurements and other smFRET assays established for bacterial transcription systems are not easily applicable to investigate comparable research question in the archaeal transcription machinery as transcriptional model systems are mainly derived from (hyper-)thermophilic archaeal organisms with an optimal reaction temperature for RNA synthesis above 60 °C. These conditions are mostly not compatible with single-molecule measurements because (i) the objective of microscopes cannot withstand such high temperatures, (ii) the fluorescent dyes used as reporters for smFRET become unstable at high temperatures or (iii) the thermal fluctuations cause too much noise in magnetic or optical tweezer experiments. However, in some instances, these obstacles were overcome. For example, sample heating devices that enabled single-molecule measurements up to 60 °C were developed that allowed to monitor TBP-induced DNA bending in real-time [21]. Here, the sample was heated via the prism that contacts the sample chamber and has not contact to the objective rather than the objective itself thereby avoiding damage of the objective. In another example, the high stability of archaeal transcription complexes once they are formed was exploited. In order to investigate the conformational state of the mobile RNAP clamp throughout the transcription cycle (see The Conformational Landscape of the RNAP Clamp section), smFRET measurements were performed at room temperature after complex formation occurred at suitable high temperatures [47].

Structural Model of the Archaeal Pre-initiation complex

While crystal structures of archaeal RNAPs have been solved [60–62], no structural information of the complete archaeal pre-initiation complex (PIC) and EC is available. Here, smFRET measurements were vital to gain insights into the structural organization of the archaeal PIC [40,42]. Due to the high sensitivity of the FRET signal to distance changes on the nanometer scale, smFRET is a valuable tool to obtain structural information. Using a network of distance constraints determined by smFRET experiments, the structure of entire multiprotein complexes can be calculated [40,63,64]. A great advantage of using this method is that even highly dynamic and flexible structures can be resolved that cannot be captured by x-ray crystallography or cryo-electron microscopy [65,66]. A method that uses probabilistic data analysis to combine single-molecule measurements with x-ray crystallography data—called the nano-positioning system (NPS)—can determine the most likely position of a fluorescent dye molecule attached to a structurally unknown part of a macromolecular complex [64]. This information can

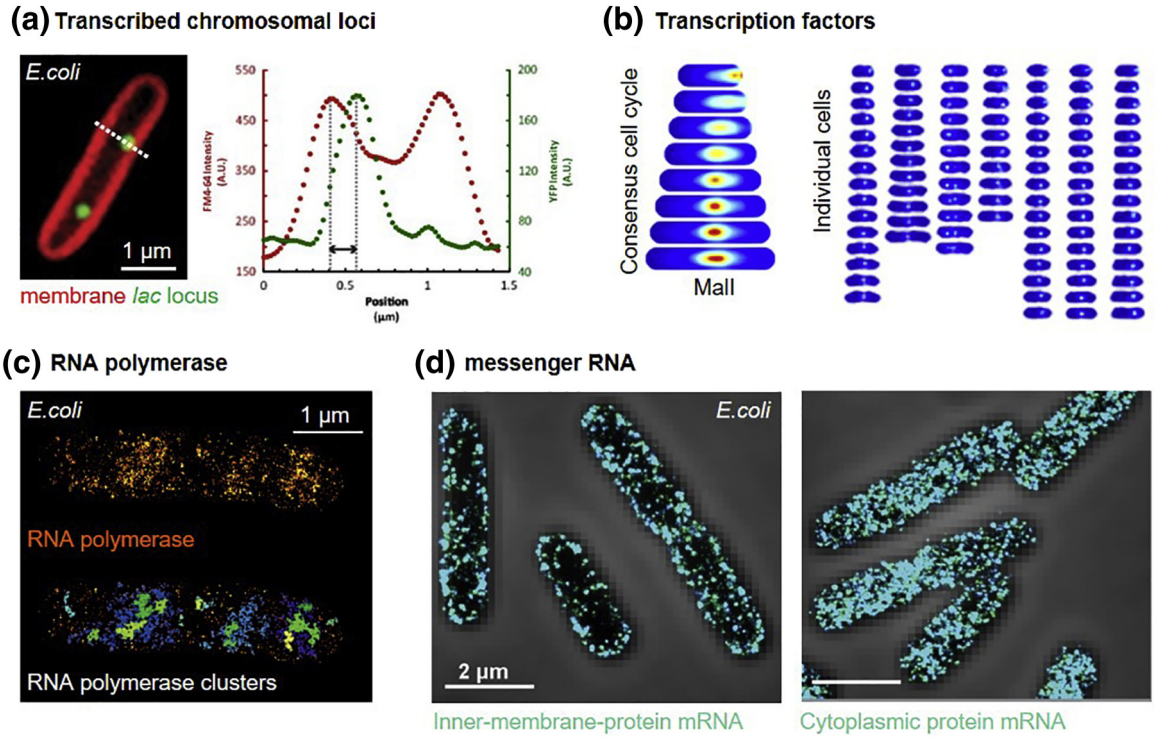

Fig. 6. Spatial organization of bacterial transcription. (a) LacY expression triggers chromosomal repositioning of the native *lac* locus (labeled with a *tetO* array) upon induction in an *E. coli* cell. Image and quantification of the distances between the chromosomal loci (green, YFP) and the membrane (red, FM4−64). Adapted from Ref. [92]. (b) MalI localization dynamics in single cells. The consensus cell cycle (left) is computed from all single-cell captures. Adapted from [93]. (c) The spatial organization of RNAPs under fast growth (LB medium) conditions in an *E. coli* cell (upper panel) is analyzed by DBScan clustering (lower panel). Adapted from Ref. [94]. (d) The *E. coli* transcriptome is spatially organized: inner-membrane-protein mRNAs (labeled by smFISH probes) have been found enriched at the membrane (left), whereas cytoplasmic protein mRNA was found distributed throughout the cell. Adapted from Ref. [95].

ultimately be used to build a structural model of a macromolecular complex. This approach was exploited to determine the interaction sites of the winged helix and zinc ribbon domain of TFE with the archaeal RNAP [42] (Fig. 4a). A few years later, based on smFRET and NPS data, a structural model of the complete open IC could be built combining over 70 distance constraints to map the position of the transcription factors TBP, TFB and TFE relative to the RNAP (Fig. 3). Moreover, the position of the highly flexible NTS was also unveiled [40]. Overall, the position of initiation factors TBP and TFB is shifted toward the stalk domain leading to a steeper entry-angle of the upstream DNA into the cleft (Fig. 3). The position of TBP is 4.5 nm apart from the eukaryotic OC. On the basis of this structural model, an interaction of the NTS with the TFB-linker-domain and the Rpo1′ rudder (a part of the largest RNAP subunit that contacts the RNA−DNA hybrid, thereby maintaining the melted upstream edge of the transcription bubble [67]) could be deduced. The structure also shows a stabilization of the downstream duplex by a lysine patch of the jaw domain. This interaction is not possible in Pol II due to steric clashes with Rpb9 and the N-terminus of Rpb5, both do not exist in most Archaea (Fig. 4b).

The Conformational Landscape of the RNAP Clamp

Structural data of the archaeal apo RNAP showed that one of the main mobile elements found in all multi-subunit RNAPs, the so-called RNAP clamp, can adopt an open and closed state [60−62]. Similar observations were made for RNAP II. Here, the clamp adopts an open state in the 10-subunit RNAP lacking subunits Rpb4/7 [68]. A closed state was found for the 12-subunit RNAP II [69,70]. The implementation of site-specific fluorescent labeling of the recombinant archaeal transcription system from *M. jannaschii* paved the way for smFRET measurements that specifically allow the observation of the conformational state of the RNAP clamp [10]. To this end, a fluorescent donor dye was engineered into the tip of the clamp coiled coil and an acceptor fluorophore was positioned in the protrusion domain that is forming one of the "crab claws" of

the RNAP thereby providing readout of the distance changes across the DNA binding channel (Fig. 5a). The recombinant transcription system furthermore provided the opportunity to mimic each step of the transcription cycle *in vitro* and to vary the composition of the transcription complexes by adding or omitting transcription factors or RNAP subunits [47]. In the absence of transcription factors, the clamp was found in two conformations at each stage of the transcription cycle (apo RNAP, IC and EC, Fig. 5b). Addition of transcription factors TFE or Spt4/5, which both bind to the clamp coiled coil but do not reach into the active site of the RNAP, shifted the equilibrium toward one of the conformations suggesting that these factors not only determine the conformational state of the clamp but stimulate the activity of the enzyme via an allosteric mechanism. Furthermore, these experiments showed that in the archaeal system, the clamp undergoes a closed-open-closed transition when the RNAP progresses from the apo enzyme to the IC and EC (Fig. 5b). TFE supports the opening of the clamp, which most likely also enables opening of the DNA. Coupled to the movement of the clamp upon TFE-stabilized promoter opening is a conformational change of the TFB linker, suggesting that the coordinated conformational changes in TFE, TFB and the RNAP eventually result in promoter opening [49]. In the elongation phase, Spt4/5 fixes the clamp in a closed conformation, thereby ensuring that the RNAP has a strong hold on the template DNA, which leads to highly processive RNA synthesis in the so-called "processive EC." A second conformation found in the EC most likely corresponds to a backtracked or paused state in which the clamp adopts a more open state as compared to the processive EC. The RNAP can be trapped in this state either artificially by omitting the NTS or when the correct nucleotide is not loaded into the active site. Possibly, this state reflects a paused state in which the DNA–RNA hybrid is tilted and which has been structurally described for bacterial as well as eukaryotic ECs. However, in these complexes, pausing factors like NusA (bacteria) or DSIIF/NELF were present, which stabilize the paused state [71,72]. Hence, it is not known whether this state can be adopted in the absence of an additional transcription factor in the archaeal EC.

Notably, not only endogenous transcription factors bind and modulate the clamp. A recent study showed that the small viral RNAP-inhibitor ORF145 targets the DNA binding channel. SmFRET measurements revealed that ORF145 arrests the clamp thereby denying access of the DNA to the RNAP [73].

A different picture of clamp dynamics, however, emerged for the bacterial RNAP. SmFRET measurements that probed the clamp conformation of *Escherichia coli* RNAP revealed that the bacterial clamp is mainly open in the apo enzyme and closes during σ70-dependent initiation [74]. Recent cryo-EM studies showed that the *Mycobacterium tuberculosis* RNAP clamp is closed in open ICs as well [75]. Further studies suggest that loading of the template strand into the RNAP active site might require transient clamp opening [76]. The clamp is found in a closed state in ECs [74]. Single-molecule measurements on immobilized molecules furthermore revealed that the clamp of the bacterial holoenzyme fluctuates dynamically between three states termed open, partly closed and closed [38].

Clamp dynamics are a conserved theme in all multi-subunit RNAPs and recent structural studies of eukaryotic RNAP I and III showed that contraction of the DNA binding cleft upon transition into the elongation phase occurs also in eukaryotic RNAPs [77–81]. However, the extent to which the clamp moves over the DNA binding channel varies with RNAP III showing extreme cleft contraction. Interestingly, RNAP I exhibits a wide range of clamp conformations in the different complexes analyzed (summarized in Ref. [82]).

Taken together, with classical structural methods failing to capture the archaeal RNAP in the different stages of transcription, smFRET measurements were crucial to reach a better understanding of the conformational dynamics of the archaeal transcription machinery, especially the RNAP clamp movements.

Utilizing Single-Molecule Methods to Study Transcription *in Vivo*

With the help of SMLM and SMT techniques, we can measure the spatial organization and dynamics of single molecules in live microbial cells at high specificity, sensitivity and spatiotemporal resolution [83–86]. This complements our knowledge of the behavior of individual molecules in the very controlled environment of *in vitro* single-molecule assays. It enables us to measure the same molecules in the complex, heterogeneous cellular environment where we can directly observe their interaction with other components of the cellular machinery.

As of today, the archaeal transcription machinery has not been studied with the help of SMLM and SMT as these methods are faced with a number of experimental challenges when applied in the extreme conditions that ensure optimal growth of archaeal organisms. On the other hand, they have been used extensively to study bacterial transcription (see recent detailed reviews [87–90]). Before discussing the technical challenges to apply single-molecule imaging to archaeal cells and which developments are required to initiate comparable studies, we would like to discuss examples from

studies on bacterial systems that illustrate the possibilities of *in vivo* single-molecule studies to enhance the understanding of transcriptional processes. In brief, studies that focused on bacterial transcription on an individual cell level have demonstrated a highly organized but dynamic intracellular organization of the components involved, namely, the transcribed genes, the RNAP and the transcription factors as well as the mRNA formed. Here, some transcribed genes were found at the periphery of the nucleoid [91,92], whereas others were found within [92] (Fig. 6a). Other studies focused on transcription factors, investigating their binding dynamics with the help of SMT [96] and using structural studies to explore their chromosomal distributions within the cells [93,97–101] (Fig. 6b). By dual-color imaging or correlated chromosome capture approaches, some transcription factors were confirmed to mediate DNA looping *in situ* [99,102]. Moreover, rapid gene regulation was observed [101]: RNAP was found either in distinct clusters or spread-out throughout the cell, depending on growth conditions or environmental cues [103–111] (Fig. 6c). Similarly, mRNA was either found scattered uniformly throughout the cell, close to the membrane or in defined loci [95,101,112,113] (Fig. 6d). Altogether, most data on prokaryotic transcription are still on a descriptive level and/or exploring only one component at a time. It therefore remains the task of future studies to establish whether the observed spatial molecular organizations are relevant for a specific biological function. To explore the interplay between the observed spatiotemporal arrangements of transcription and other possible influences (e.g., expression levels and DNA-binding behavior of transcription factors, the three-dimensional architecture and local domains of the nucleoid or co-occurring replication and translation), advanced multi-color SMLM imaging and co-tracking schemes for living cells are needed. However, the development of these techniques is still in its infancy [86]. With these at hand, it will be possible to verify current hypotheses and models, for example, that observed spatial patterns might form due to co-regulated genes and/or in respect to varying transcriptional activities. This could, for example, answer the question if the RNAP clusters forming under fast growth conditions are engaged in rRNA synthesis as suggested by the high transcription levels of ribosomal RNA under these conditions [114]. In this case, it still remains to be experimentally shown that the rRNA operons co-localize with the RNAP clusters *in vivo*, a hypothesis that is currently subject of considerable debate [115].

Likewise, correlative techniques, for example, correlative *in vivo* single-molecule fluorescence and electron microscopy studies, might play an essential role in the future. Here, electron microscopy yields detailed, high-resolution images of subcellular ultrastructure but misses the specific contrast of fluorescence microscopy, which on the other hand can provide details about the organization and cellular dynamics of specific, single molecules with nanometer resolution. Such correlative studies are not established for Archaea, yet but a few studies were undertaken in Bacteria [116–118].

Thus, which are the methodological improvements needed when addressing similar questions in Archaea? Prokaryotes in general are more challenging to address by advanced microscopic techniques than most common mammalian cells as they are comparatively small. Moreover, prokaryotic cells are compact single-cell organisms protected by robust cell hulls with rather low protein abundances and fast growth rates [86]. Archaeal cells are even more challenging as they typically live in extreme habitats, for example, at high or very low temperature or in high saline, acidic, alkaline or anaerobe environments, and in many cases, the exact conditions for their cultivation remain unknown. Furthermore, many Archaea produce colorful pigments, for example, rhodopsins or carotenoids, which cause strong autofluorescence. In addition, for many Archaea, no adequate set of genetic tools exists [119]. This severely constraints the choice of suitable fluorescent reporters and labeling approaches, which are already limited to a special group of SMLM-suitable photoswitching fluorophores and inert, highly specific labels [86,120]: First, the autofluorescence blocks large spectral ranges. To counteract this, several options can be explored, for example, in case of halophiles, choosing/developing fluorescent proteins that exhibit higher solubility or are red-shifted [121–123]. Also, pigment-free mutants might be a good option, like, for example, a colorless *Haloferax volcanii* strain developed by interrupting the carotenoid synthesis pathway [124]. Second, most fluorophores and SMLM-photoswitching mechanisms are very sensitive to the surrounding conditions. This needs to be taken into account when choosing fluorescent tags for a given Archaeon. For instance, fluorescent proteins cannot mature under anaerobic conditions [125], fluorophore brightness at a specific pH depends on the chromophores pKa value (which therefore should be rather low for acidic pH environments [126]) and most organic dyes need a neutral pH for proper photoswitching [127]. A third, fundamental choice is whether to use intrinsic or extrinsic labeling strategies: Intrinsic strategies (using enzyme, peptide or fluorescent protein tags) depend on genetic engineering tools, which are currently not established for most Archaea but offer a high specificity. Even for frequently studied archaeal families, most available genetic tools are rather recent developments, like, for example, selection strains and plasmid systems for halophiles [128], a

heat-stable protein tag [129] and strains that allow the incorporation of nucleoside analogs during DNA replication [130] for hyperthermophiles. Furthermore, intrinsic tags might not fold properly when expressed in non-native intracellular environments [123] and might need codon optimization [131]. Extrinsic labels on the other hand need to pass cell barriers like cell walls and membranes to reach their target. This can be achieved, for example, by utilizing small and membrane-permeable stains [121,129,132], fixing and permeabilizing the cells for immunofluorescence [130,133–135] or by actively using the dye's non-permeability as a feature to stain the cell wall [136]. Extracellular tags should also be checked for their ability to function under the conditions at hand, for example, in a high-salt environment [132]. Notably, established protocols for the fixation of archaea are still rather scarce and Archaea are enveloped by the S-layer, which differs significantly from the bacterial cell wall. On the other hand, recent developments in fabricating customized microfluidics and temperature-isolating stages allow to grow Archaea in their preferred extreme environments on the microscope [137]. Finally, when aiming at measuring single-molecule dynamics, intracellular charges become important. For instance, for *H. volcanii*, effects of differently charged fluorescent protein surfaces alter the observed diffusion coefficient: Positively charged proteins were found to diffuse significantly slower than negatively charged and neutral proteins [131].

Nevertheless, even with all these technical obstacles, studying the archaeal world by SMLM and SMT technologies is not completely out-of-sight. With the help of optimizations in current methodologies and possibly improvements of fluorophores and labeling systems, we expect the first observations of single molecules in living Archaea to occur rather sooner than later. This will open the large and exciting field of accessing the archaeal biology at a single-molecule level *in vivo*, especially their unique transcription machinery.

Acknowledgments

We apologize to those whose work we were unable to cite owing to space constraints. The authors thank the "archaeal transcription group" at the Institute of Microbiology at the University of Regensburg (Felix Grünberger, Winfried Hausner, Robert Reichelt). We gratefully acknowledge financial support by the Deutsche Forschungsgemeinschaft (DFG grant no. SFB960-TP7 to D.G.). U.E. acknowledges funding by the Max Planck Society, SYNMIKRO and the Deutsche Forschungsgemeinschaft (SPP 2141, project 405974843).

Received 11 April 2019;
Received in revised form 27 May 2019;
Available online 15 June 2019

Keywords:
Archaea;
single-molecule FRET;
nano-positioning system;
single-molecule localization microscopy;
RNA polymerase

Abbreviations used:
RNAP, RNA polymerase; SMLM, single-molecule localization microscopy; SMT, single-molecule tracking; BRE, B recognition element; TBP, TATA-binding protein; TFB, transcription factor B; IC, initiation complex; EC, elongation complex; NTS, non-template strand; NPS, nano-positioning system; PIC, pre-initiation complex.

References

[1] F. Werner, D. Grohmann, Evolution of multisubunit RNA polymerases in the three domains of life, Nat. Rev. Microbiol. 9 (2011) 85–98, https://doi.org/10.1038/nrmicro2507.
[2] S.-H. Jun, M.J. Reichlen, M. Tajiri, K.S. Murakami, Archaeal RNA polymerase and transcription regulation, Crit. Rev. Biochem. Mol. Biol. 46 (2011) 27–40, https://doi.org/10.3109/10409238.2010.538662.
[3] J. Griesenbeck, H. Tschochner, D. Grohmann, Macromolecular Protein Complexes, Springer International Publishing, Cham, 2017, https://doi.org/10.1007/978-3-319-46503-6.
[4] M. Dangkulwanich, T. Ishibashi, L. Bintu, C. Bustamante, Molecular mechanisms of transcription through single-molecule experiments, Chem. Rev. 114 (2014) 3203–3223, https://doi.org/10.1021/cr400730x.
[5] L. Bai, T.J. Santangelo, M.D. Wang, Single-molecule analysis of RNA polymerase transcription, Annu. Rev. Biophys. Biomol. Struct. 35 (2006) 343–360, https://doi.org/10.1146/annurev.biophys.35.010406.150153.
[6] J. Gelles, R. Landick, RNA polymerase as a molecular motor, Cell. 93 (1998) 13–16, https://doi.org/10.1016/S0092-8674(00)81140-X.
[7] M.H. Larson, R. Landick, S.M. Block, Single-molecule studies of RNA polymerase: one singular sensation, every little step it takes, Mol. Cell 41 (2011) 249–262, https://doi.org/10.1016/j.molcel.2011.01.008.
[8] D.A. Schafer, J. Gelles, M.P. Sheetz, R. Landick, Transcription by single molecules of RNA polymerase observed by light microscopy, Nature. 352 (1991) 444–448, https://doi.org/10.1038/352444a0.
[9] J. Michaelis, B. Treutlein, Single-molecule studies of RNA polymerases, Chem. Rev. 113 (2013) 8377–8399, https://doi.org/10.1021/cr400207r.
[10] S. Schulz, K. Kramm, F. Werner, D. Grohmann, Fluorescently labeled recombinant RNAP system to probe archaeal transcription initiation, Methods. 86 (2015) 10–18, https://doi.org/10.1016/j.ymeth.2015.04.017.
[11] P. Schluesche, G. Heiss, M. Meisterernst, D.C. Lamb, Dynamics of TBP binding to the TATA box, in: J. Enderlein,

Z.K. Gryczynski, R. Erdmann (Eds.), International Society for Optics and Photonics, 2008, 68620E, https://doi.org/10.1117/12.769177.
[12] A.N. Kapanidis, Y.W. Ebright, R.D. Ludescher, S. Chan, R.H. Ebright, Mean DNA bend angle and distribution of DNA bend angles in the CAP–DNA complex in solution, J. Mol. Biol. 312 (2001) 453–468, https://doi.org/10.1006/jmbi.2001.4976.
[13] K. Smollett, F. Blombach, R. Reichelt, M. Thomm, F. Werner, A global analysis of transcription reveals two modes of Spt4/5 recruitment to archaeal RNA polymerase, Nat. Microbiol. 2 (2017), 17021, https://doi.org/10.1038/nmicrobiol.2017.21.
[14] D.B. Nikolov, S.H. Hu, J. Lin, A. Gasch, A. Hoffmann, M. Horikoshi, N.H. Chua, R.G. Roeder, S.K. Burley, Crystal structure of TFIID TATA-box binding protein, Nature. 360 (1992) 40–46, https://doi.org/10.1038/360040a0.
[15] B.L. Davison, J.-M. Egly, E.R. Mulvihill, P. Chambon, Formation of stable preinitiation complexes between eukaryotic class B transcription factors and promoter sequences, Nature. 301 (1983) 680–686, https://doi.org/10.1038/301680a0.
[16] S.D. Bell, P.L. Kosa, P.B. Sigler, S.P. Jackson, Orientation of the transcription preinitiation complex in archaea, Proc. Natl. Acad. Sci. U. S. A. 96 (1999) 13662–13667, https://doi.org/10.1073/PNAS.96.24.13662.
[17] W. Hausner, J. Wettach, C. Hethke, M. Thomm, Two transcription factors related with the eucaryal transcription factors TATA-binding protein and transcription factor IIB direct promoter recognition by an archaeal RNA polymerase, J. Biol. Chem. 271 (1996) 30144–30148, https://doi.org/10.1074/JBC.271.47.30144.
[18] K. Kramm, C. Engel, D. Grohmann, Transcription initiation factor TBP: old friend new questions, Biochem. Soc. Trans. (2019), BST20180623, https://doi.org/10.1042/BST20180623.
[19] F. Werner, R.O.J. Weinzierl, Direct modulation of RNA polymerase core functions by basal transcription factors, Mol. Cell. Biol. 25 (2005) 8344–8355, https://doi.org/10.1128/MCB.25.18.8344-8355.2005.
[20] S.C. Wiesler, R.O.J. Weinzierl, The linker domain of basal transcription factor TFIIB controls distinct recruitment and transcription stimulation functions, Nucleic Acids Res. 39 (2011) 464–474, https://doi.org/10.1093/nar/gkq809.
[21] A. Gietl, P. Holzmeister, F. Blombach, S. Schulz, L.V. von Voithenberg, D.C. Lamb, F. Werner, P. Tinnefeld, D. Grohmann, Eukaryotic and archaeal TBP and TFB/TF(II)B follow different promoter DNA bending pathways, Nucleic Acids Res. 42 (2014) 6219–6231, https://doi.org/10.1093/nar/gku273.
[22] R.H. Blair, J.A. Goodrich, J.F. Kugel, Single-molecule fluorescence resonance energy transfer shows uniformity in TATA binding protein-induced DNA bending and heterogeneity in bending kinetics, Biochemistry. 51 (2012) 7444–7455, https://doi.org/10.1021/bi300491j.
[23] G. Heiss, E. Ploetz, L. Voith von Voithenberg, R. Viswanathan, S. Glaser, P. Schluesche, S. Madhira, M. Meisterernst, D.T. Auble, D.C. Lamb, Conformational changes and catalytic inefficiency associated with Mot1-mediated TBP–DNA dissociation, Nucleic Acids Res. (2019), https://doi.org/10.1093/nar/gky1322.
[24] P. Schluesche, G. Stelzer, E. Piaia, D.C. Lamb, M. Meisterernst, NC2 mobilizes TBP on core promoter TATA boxes, Nat. Struct. Mol. Biol. 14 (2007) 1196–1201, https://doi.org/10.1038/nsmb1328.
[25] F. Blombach, D. Grohmann, Same same but different: the evolution of TBP in archaea and their eukaryotic offspring, Transcription. 8 (2017) 162–168, https://doi.org/10.1080/21541264.2017.1289879.
[26] G.A. Patikoglou, J.L. Kim, L. Sun, S.H. Yang, T. Kodadek, S.K. Burley, TATA element recognition by the TATA box-binding protein has been conserved throughout evolution, Genes Dev. 13 (1999) 3217–3230. http://www.ncbi.nlm.nih.gov/pubmed/10617571 (accessed August 20, 2018).
[27] G.M. Perez-Howard, P.A. Weil, J.M. Beechem, Yeast TATA binding protein interaction with DNA: fluorescence determination of oligomeric state, equilibrium binding, on-rate, and dissociation kinetics, Biochemistry. 34 (1995) 8005–8017, https://doi.org/10.1021/bi00025a006.
[28] R.O. Sprouse, I. Shcherbakova, H. Cheng, E. Jamison, M. Brenowitz, D.T. Auble, Function and structural organization of Mot1 bound to a natural target promoter, J. Biol. Chem. 283 (2008) 24935–24948, https://doi.org/10.1074/jbc.M803749200.
[29] Y. Kim, J.H. Geiger, S. Hahn, P.B. Sigler, Crystal structure of a yeast TBP/TATA-box complex, Nature. 365 (1993) 512–520, https://doi.org/10.1038/365512a0.
[30] J. Gouge, N. Guthertz, K. Kramm, O. Dergai, G. Abascal-Palacios, K. Satia, P. Cousin, N. Hernandez, D. Grohmann, A. Vannini, Molecular mechanisms of Bdp1 in TFIIIB assembly and RNA polymerase III transcription initiation, Nat. Commun. 8 (2017), 130, https://doi.org/10.1038/s41467-017-00126-1.
[31] P.C. Nickels, B. Wünsch, P. Holzmeister, W. Bae, L.M. Kneer, D. Grohmann, P. Tinnefeld, T. Liedl, Molecular force spectroscopy with a DNA origami-based nanoscopic force clamp, Science. 354 (2016) 305–307, https://doi.org/10.1126/science.aah5974.
[32] J.J. Funke, P. Ketterer, C. Lieleg, S. Schunter, P. Korber, H. Dietz, Uncovering the forces between nucleosomes using DNA origami, Sci. Adv. 2 (2016), e1600974, https://doi.org/10.1126/sciadv.1600974.
[33] B. Henneman, R. T. Dame, Archaeal histones: dynamic and versatile genome architects, AIMS Microbiol. 1 (2015) 72–81, https://doi.org/10.3934/microbiol.2015.1.72.
[34] F. Mattiroli, S. Bhattacharyya, P.N. Dyer, A.E. White, K. Sandman, B.W. Burkhart, K.R. Byrne, T. Lee, N.G. Ahn, T.J. Santangelo, J.N. Reeve, K. Luger, Structure of histone-based chromatin in Archaea, Science. 357 (2017) 609–612, https://doi.org/10.1126/science.aaj1849.
[35] E. Peeters, R.P.C. Driessen, F. Werner, R.T. Dame, The interplay between nucleoid organization and transcription in archaeal genomes, Nat. Rev. Microbiol. 13 (2015) 333–341, https://doi.org/10.1038/nrmicro3467.
[36] Y. Alhadid, S. Chung, E. Lerner, D.J. Taatjes, S. Borukhov, S. Weiss, Studying transcription initiation by RNA polymerase with diffusion-based single-molecule fluorescence, Protein Sci. 26 (2017) 1278–1290, https://doi.org/10.1002/pro.3160.
[37] T. Cordes, Y. Santoso, A.I. Tomescu, K. Gryte, L.C. Hwang, B. Camará, S. Wigneshweraraj, A.N. Kapanidis, Sensing DNA opening in transcription using quenchable Förster resonance energy transfer, Biochemistry. 49 (2010) 9171–9180, https://doi.org/10.1021/bi101184g.
[38] D. Duchi, K. Gryte, N.C. Robb, Z. Morichaud, C. Sheppard, K. Brodolin, S. Wigneshweraraj, A.N. Kapanidis, Conformational heterogeneity and bubble dynamics in single bacterial transcription initiation complexes, Nucleic Acids Res. 46 (2018) 677–688, https://doi.org/10.1093/nar/gkx1146.

[39] K. Brodolin, Antibiotics trapping transcription initiation intermediates. To melt or to bend, what's first? Transcription. 2 (2011) 60–65, https://doi.org/10.4161/trns.2.2.14366.
[40] J. Nagy, D. Grohmann, A.C.M. Cheung, S. Schulz, K. Smollett, F. Werner, J. Michaelis, Complete architecture of the archaeal RNA polymerase open complex from single-molecule FRET and NPS, Nat. Commun. 6 (2015), 6161, https://doi.org/10.1038/ncomms7161.
[41] Y. He, C. Yan, J. Fang, C. Inouye, R. Tjian, I. Ivanov, E. Nogales, Near-atomic resolution visualization of human transcription promoter opening, Nature. 533 (2016) 359–365, https://doi.org/10.1038/nature17970.
[42] D. Grohmann, J. Nagy, A. Chakraborty, D. Klose, D. Fielden, R.H. Ebright, J. Michaelis, F. Werner, The initiation factor TFE and the elongation factor Spt4/5 compete for the RNAP clamp during transcription initiation and elongation, Mol. Cell 43 (2011) 263–274, https://doi.org/10.1016/j.molcel.2011.05.030.
[43] F. Blombach, E. Salvadori, T. Fouqueau, J. Yan, J. Reimann, C. Sheppard, K.L. Smollett, S.V. Albers, C.W.M. Kay, K. Thalassinos, F. Werner, Archaeal TFEα/β is a hybrid of TFIIE and the RNA polymerase III subcomplex hRPC62/39, Elife. 4 (2015), e08378, https://doi.org/10.7554/eLife.08378.
[44] S. Grünberg, M.S. Bartlett, S. Naji, M. Thomm, Transcription factor E is a part of transcription elongation complexes, J. Biol. Chem. 282 (2007) 35482–35490, https://doi.org/10.1074/jbc.M707371200.
[45] P. Spitalny, M. Thomm, Analysis of the open region and of DNA-protein contacts of archaeal RNA polymerase transcription complexes during transition from initiation to elongation, J. Biol. Chem. 278 (2003) 30497–30505, https://doi.org/10.1074/jbc.M303633200.
[46] F. Blombach, K.L. Smollett, D. Grohmann, F. Werner, Molecular mechanisms of transcription initiation—structure, function, and evolution of TFE/TFIIE-like factors and open complex formation, J. Mol. Biol. 428 (2016) 2592–2606, https://doi.org/10.1016/j.jmb.2016.04.016.
[47] S. Schulz, A. Gietl, K. Smollett, P. Tinnefeld, F. Werner, D. Grohmann, TFE and Spt4/5 open and close the RNA polymerase clamp during the transcription cycle, Proc. Natl. Acad. Sci. U. S. A. 113 (2016) E1816–E1825, https://doi.org/10.1073/pnas.1515817113.
[48] D. Kostrewa, M.E. Zeller, K.-J. Armache, M. Seizl, K. Leike, M. Thomm, P. Cramer, RNA polymerase II–TFIIB structure and mechanism of transcription initiation, Nature. 462 (2009) 323–330, https://doi.org/10.1038/nature08548.
[49] S. Dexl, R. Reichelt, K. Kraatz, S. Schulz, D. Grohmann, M. Bartlett, M. Thomm, Displacement of the transcription factor B reader domain during transcription initiation, Nucleic Acids Res. 46 (2018) 10066–10081, https://doi.org/10.1093/nar/gky699.
[50] A.J. Carpousis, J.D. Gralla, Cycling of ribonucleic acid polymerase to produce oligonucleotides during initiation in vitro at the lac UV5 promoter, Biochemistry. 19 (1980) 3245–3253, https://doi.org/10.1021/bi00555a023.
[51] M.A. Grachev, E.F. Zaychikov, Initiation by Escherichia coli RNA-polymerase: transformation of abortive to productive complex, FEBS Lett. 115 (1980) 23–26. http://www.ncbi.nlm.nih.gov/pubmed/6156091.
[52] L.M. Munson, W.S. Reznikoff, Abortive initiation and long RNA synthesis, Biochemistry. 20 (1981) 2081–2085, https://doi.org/10.1021/bi00511a003.
[53] A. Revyakin, C. Liu, R.H. Ebright, T.R. Strick, Abortive initiation and productive initiation by RNA polymerase involve DNA scrunching, Science. 314 (2006) 1139–1143, https://doi.org/10.1126/science.1131398.
[54] A.N. Kapanidis, E. Margeat, S.O. Ho, E. Kortkhonjia, S. Weiss, R.H. Ebright, Initial transcription by RNA polymerase proceeds through a DNA-scrunching mechanism, Science. 36 (2006) 3809–3823, https://doi.org/10.1126/science.1131399.
[55] F. Blombach, T. Daviter, D. Fielden, D. Grohmann, K. Smollett, F. Werner, Archaeology of RNA polymerase: factor swapping during the transcription cycle, Biochem. Soc. Trans. 41 (2013) 362–367, https://doi.org/10.1042/BST20120274.
[56] A. Hirtreiter, G.E. Damsma, A.C.M. Cheung, D. Klose, D. Grohmann, E. Vojnic, A.C.R. Martin, P. Cramer, F. Werner, Spt4/5 stimulates transcription elongation through the RNA polymerase clamp coiled-coil motif, Nucleic Acids Res. 38 (2010) 4040–4051, https://doi.org/10.1093/nar/gkq135.
[57] E. Lerner, S. Chung, B.L. Allen, S. Wang, J. Lee, S.W. Lu, L.W. Grimaud, A. Ingargiola, X. Michalet, Y. Alhadid, S. Borukhov, T.R. Strick, D.J. Taatjes, S. Weiss, Backtracked and paused transcription initiation intermediate of Escherichia coli RNA polymerase., Proc. Natl. Acad. Sci. U. S. A. 113 (2016) E6562–E6571. doi:10.1073/pnas.1605038113.
[58] D. Dulin, D.L.V. Bauer, A.M. Malinen, J.J.W. Bakermans, M. Kaller, Z. Morichaud, I. Petushkov, M. Depken, K. Brodolin, A. Kulbachinskiy, A.N. Kapanidis, Pausing controls branching between productive and non-productive pathways during initial transcription in bacteria, Nat. Commun. 9 (2018), 1478, https://doi.org/10.1038/s41467-018-03902-9.
[59] D. Duchi, D.L.V. Bauer, L. Fernandez, G. Evans, N. Robb, L.C. Hwang, K. Gryte, A. Tomescu, P. Zawadzki, Z. Morichaud, K. Brodolin, A.N. Kapanidis, RNA polymerase pausing during initial transcription, Mol. Cell 63 (2016) 939–950, https://doi.org/10.1016/J.MOLCEL.2016.08.011.
[60] S.-H. Jun, A. Hirata, T. Kanai, T.J. Santangelo, T. Imanaka, K.S. Murakami, The x-ray crystal structure of the euryarchaeal RNA polymerase in an open-clamp configuration, Nat. Commun. 5 (2014), 5132, https://doi.org/10.1038/ncomms6132.
[61] A. Hirata, B.J. Klein, K.S. Murakami, The x-ray crystal structure of RNA polymerase from Archaea, Nature. 451 (2008) 851–854, https://doi.org/10.2210/PDB3HKZ/PDB.
[62] M.N. Wojtas, M. Mogni, O. Millet, S.D. Bell, N.G.A. Abrescia, Structural and functional analyses of the interaction of archaeal RNA polymerase with DNA, Nucleic Acids Res. 40 (2012) 9941, https://doi.org/10.2210/PDB4AYB/PDB.
[63] B. Treutlein, A. Muschielok, J. Andrecka, A. Jawhari, C. Buchen, D. Kostrewa, F. Hög, P. Cramer, J. Michaelis, Dynamic architecture of a minimal RNA polymerase II open promoter complex, Mol. Cell 46 (2012) 136–146, https://doi.org/10.1016/j.molcel.2012.02.008.
[64] A. Muschielok, J. Andrecka, A. Jawhari, F. Brückner, P. Cramer, J. Michaelis, A nano-positioning system for macromolecular structural analysis, Nat. Methods 5 (2008) 965–971, https://doi.org/10.1038/nmeth.1259.
[65] J. Andrecka, R. Lewis, F. Brückner, E. Lehmann, P. Cramer, J. Michaelis, Single-molecule tracking of mRNA exiting from RNA polymerase II, Proc. Natl. Acad. Sci. U. S. A. 105 (2008) 135–140, https://doi.org/10.1073/pnas.0703815105.
[66] J. Andrecka, B. Treutlein, M.A.I. Arcusa, A. Muschielok, R. Lewis, A.C.M. Cheung, P. Cramer, J. Michaelis, Nano positioning system reveals the course of upstream and

nontemplate DNA within the RNA polymerase II elongation complex, Nucleic Acids Res. 37 (2009) 5803–5809, https://doi.org/10.1093/nar/gkp601.
[67] C.O. Barnes, M. Calero, I. Malik, B.W. Graham, H. Spahr, G. Lin, A.E. Cohen, I.S. Brown, Q. Zhang, F. Pullara, M.A. Trakselis, C.D. Kaplan, G. Calero, Crystal structure of a transcribing RNA polymerase II complex reveals a complete transcription bubble, Mol. Cell 59 (2015) 258–269, https://doi.org/10.1016/j.molcel.2015.06.034.
[68] P. Cramer, D.A. Bushnell, R.D. Kornberg, Structural basis of transcription: RNA polymerase II at 2.8 angstrom resolution, Science. 292 (2001) 1863–1876, https://doi.org/10.1126/science.1059493.
[69] K.-J. Armache, H. Kettenberger, P. Cramer, Architecture of initiation-competent 12-subunit RNA polymerase II, Proc. Natl. Acad. Sci. 100 (2003) 6964–6968, https://doi.org/10.1073/pnas.1030608100.
[70] D.A. Bushnell, R.D. Kornberg, Complete, 12-subunit RNA polymerase II at 4.1-Å resolution: implications for the initiation of transcription, Proc. Natl. Acad. Sci. 100 (2003) 6969–6973, https://doi.org/10.1073/pnas.1130601100.
[71] S.M. Vos, L. Farnung, H. Urlaub, P. Cramer, Structure of paused transcription complex Pol II–DSIF–NELF, Nature. 560 (2018) 601–606, https://doi.org/10.1038/s41586-018-0442-2.
[72] X. Guo, A.G. Myasnikov, J. Chen, C. Crucifix, G. Papai, M. Takacs, P. Schultz, A. Weixlbaumer, Structural basis for NusA stabilized transcriptional pausing, Mol. Cell 69 (2018) 816–827.e4, https://doi.org/10.1016/j.molcel.2018.02.008.
[73] C. Sheppard, F. Blombach, A. Belsom, S. Schulz, T. Daviter, K. Smollett, E. Mahieu, S. Erdmann, P. Tinnefeld, R. Garrett, D. Grohmann, J. Rappsilber, F. Werner, Repression of RNA polymerase by the archaeo-viral regulator ORF145/RIP, Nat. Commun. 7 (2016), 13595, https://doi.org/10.1038/ncomms13595.
[74] A. Chakraborty, D. Wang, Y.W. Ebright, Y. Korlann, E. Kortkhonjia, T. Kim, S. Chowdhury, S. Wigneshweraraj, H. Irschik, R. Jansen, B.T. Nixon, J. Knight, S. Weiss, R.H. Ebright, Opening and closing of the bacterial RNA polymerase clamp, Science. 337 (2012) 591–595, https://doi.org/10.1126/science.1218716.
[75] H. Boyaci, J. Chen, R. Jansen, S.A. Darst, E.A. Campbell, Structures of an RNA polymerase promoter melting intermediate elucidate DNA unwinding, Nature. 565 (2019) 382–385, https://doi.org/10.1038/s41586-018-0840-5.
[76] A. Feklistov, B. Bae, J. Hauver, A. Lass-Napiorkowska, M. Kalesse, F. Glaus, K.-H. Altmann, T. Heyduk, R. Landick, S.A. Darst, RNA polymerase motions during promoter melting, Science 356 (2017) 863–866., https://doi.org/10.1126/science.aam7858.
[77] C. Engel, T. Gubbey, S. Neyer, S. Sainsbury, C. Oberthuer, C. Baejen, C. Bernecky, P. Cramer, Structural basis of RNA polymerase I transcription initiation, Cell. 169 (2017) 120–131.e22, https://doi.org/10.1016/j.cell.2017.03.003.
[78] E. Torreira, J.A. Louro, I. Pazos, N. González-Polo, D. Gil-Carton, A.G. Duran, S. Tosi, O. Gallego, O. Calvo, C. Fernández-Tornero, The dynamic assembly of distinct RNA polymerase I complexes modulates rDNA transcription, Elife. 6 (2017), https://doi.org/10.7554/eLife.20832.
[79] C. Fernández-Tornero, M. Moreno-Morcillo, U.J. Rashid, N.M.I. Taylor, F.M. Ruiz, T. Gruene, P. Legrand, U. Steuerwald, C.W. Müller, Crystal structure of the 14-subunit RNA polymerase I, Nature. 502 (2013) 644–649, https://doi.org/10.1038/nature12636.
[80] G. Abascal-Palacios, E.P. Ramsay, F. Beuron, E. Morris, A. Vannini, Structural basis of RNA polymerase III transcription initiation, Nature. 553 (2018) 301–306, https://doi.org/10.1038/nature25441.
[81] A. Vannini, P. Cramer, Conservation between the RNA polymerase I, II, and III transcription initiation machineries, Mol. Cell 45 (2012) 439–446, https://doi.org/10.1016/j.molcel.2012.01.023.
[82] C. Engel, S. Neyer, P. Cramer, Distinct mechanisms of transcription initiation by RNA polymerases I and II, Annu. Rev. Biophys. 47 (2018) 425–446, https://doi.org/10.1146/annurev-biophys-070317-033058.
[83] A. Gahlmann, W.E. Moerner, Exploring bacterial cell biology with single-molecule tracking and super-resolution imaging, Nat Rev Microbiol. 12 (2014) 9–22, https://doi.org/10.1038/nrmicro3154.
[84] A.N. Kapanidis, A. Lepore, M. El Karoui, Rediscovering bacteria through single-molecule imaging in living cells, Biophys. J. 115 (2018) 190–202, https://doi.org/10.1016/j.bpj.2018.03.028.
[85] J. Elf, I. Barkefors, Single-molecule kinetics in living cells, Annu. Rev. Biochem. 88 (2019) annurev-biochem-013118-110801. doi:10.1146/annurev-biochem-013118-110801.
[86] I. Vojnovic, J. Winkelmeier, U. Endesfelder, Visualizing the inner life of microbes: practices of multi-color single molecule localization microscopy in microbiology, Biochem. Soc. Trans. in publica (2019), https://doi.org/10.1042/BST20180399.
[87] X. Weng, J. Xiao, Spatial organization of transcription in bacterial cells, Trends Genet. 30 (2014) 287–297, https://doi.org/10.1016/j.tig.2014.04.008.
[88] S. Bakshi, H. Choi, J.C. Weisshaar, The spatial biology of transcription and translation in rapidly growing Escherichia coli, Front. Microbiol. 6 (2015), 636, https://doi.org/10.3389/fmicb.2015.00636.
[89] L.A. van Gijtenbeek, J. Kok, Illuminating messengers: an update and outlook on RNA visualization in bacteria, Front. Microbiol. 8 (2017), 1161, https://doi.org/10.3389/fmicb.2017.01161.
[90] D.J. Jin, C. Mata Martin, Z. Sun, C. Cagliero, Y.N. Zhou, Nucleolus-like compartmentalization of the transcription machinery in fast-growing bacterial cells, Crit. Rev. Biochem. Mol. Biol. 52 (2017) 96–106, https://doi.org/10.1080/10409238.2016.1269717.
[91] M.A. Sanchez-Romero, D.J. Lee, E. Sanchez-Moran, S.J. Busby, Location and dynamics of an active promoter in Escherichia coli K-12, Biochem. J. 441 (2012) 481–485, https://doi.org/10.1042/BJ20111258.
[92] E.A. Libby, M. Roggiani, M. Goulian, Membrane protein expression triggers chromosomal locus repositioning in bacteria, Proc. Natl. Acad. Sci. U. S. A. 109 (2012) 7445–7450, https://doi.org/10.1073/pnas.1109479109.
[93] N.J. Kuwada, B. Traxler, P.A. Wiggins, Genome-scale quantitative characterization of bacterial protein localization dynamics throughout the cell cycle, Mol. Microbiol. 95 (2015) 64–79, https://doi.org/10.1111/mmi.12841.
[94] U. Endesfelder, Hochaufgelöste Zellbiologie, BIOspektrum. 22 (2016) 217, https://doi.org/10.1007/s12268-016-0675-2.
[95] J.R. Moffitt, S. Pandey, A.N. Boettiger, S. Wang, X. Zhuang, Spatial organization shapes the turnover of a bacterial transcriptome, Elife. 5 (2016), https://doi.org/10.7554/eLife.13065.

[96] J. Elf, G.W. Li, X.S. Xie, Probing transcription factor dynamics at the single-molecule level in a living cell, Science. 316 (2007) 1191–1194, https://doi.org/10.1126/science.1141967.
[97] W. Wang, G.W. Li, C. Chen, X.S. Xie, X. Zhuang, Chromosome organization by a nucleoid-associated protein in live bacteria, Science. 333 (2011) 1445–1449, https://doi.org/10.1126/science.1204697.
[98] S.F. Lee, M.A. Thompson, M.A. Schwartz, L. Shapiro, W.E. Moerner, Super-resolution imaging of the nucleoid-associated protein HU in Caulobacter crescentus, Biophys. J. 100 (2011) L31–L33, https://doi.org/10.1016/j.bpj.2011.02.022.
[99] Z. Qian, E.K. Dimitriadis, R. Edgar, P. Eswaramoorthy, S. Adhya, Galactose repressor mediated intersegmental chromosomal connections in Escherichia coli, Proc. Natl. Acad. Sci. U. S. A. 109 (2012) 11336–11341, https://doi.org/10.1073/pnas.1208595109.
[100] T.E. Kuhlman, E.C. Cox, Gene location and DNA density determine transcription factor distributions in Escherichia coli, Mol. Syst. Biol. 8 (2012), 610, https://doi.org/10.1038/msb.2012.42.
[101] L.A. Sepulveda, H. Xu, J. Zhang, M.Y. Wang, I. Golding, Measurement of gene regulation in individual cells reveals rapid switching between promoter states, Science. 351 (2016) 1218–1222, https://doi.org/10.1126/science.aad0635.
[102] Z. Hensel, X. Weng, A.C. Lagda, J. Xiao, Transcription-factor-mediated DNA looping probed by high-resolution, single-molecule imaging in live E. coli cells, PLoS Biol. 11 (2013), e1001591, https://doi.org/10.1371/journal.pbio.1001591.
[103] P.J. Lewis, S.D. Thaker, J. Errington, Compartmentalization of transcription and translation in Bacillus subtilis, EMBO J. 19 (2000) 710–718, https://doi.org/10.1093/emboj/19.4.710.
[104] J.E. Cabrera, D.J. Jin, The distribution of RNA polymerase in Escherichia coli is dynamic and sensitive to environmental cues, Mol. Microbiol. 50 (2003) 1493–1505, https://doi.org/10.1046/j.1365-2958.2003.03805.x.
[105] D.J. Jin, J.E. Cabrera, Coupling the distribution of RNA polymerase to global gene regulation and the dynamic structure of the bacterial nucleoid in Escherichia coli, J. Struct. Biol. 156 (2006) 284–291, https://doi.org/10.1016/j.jsb.2006.07.005.
[106] B.P. Bratton, R.A. Mooney, J.C. Weisshaar, Spatial distribution and diffusive motion of RNA polymerase in live Escherichia coli, J. Bacteriol. 193 (2011) 5138–5146, https://doi.org/10.1128/JB.00198-11.
[107] S. Bakshi, A. Siryaporn, M. Goulian, J.C. Weisshaar, Superresolution imaging of ribosomes and RNA polymerase in live Escherichia coli cells, Mol. Microbiol. 85 (2012) 21–38, https://doi.org/10.1111/j.1365-2958.2012.08081.x.
[108] U. Endesfelder, K. Finan, S.J. Holden, P.R. Cook, A.N. Kapanidis, M. Heilemann, Multiscale spatial organization of RNA polymerase in Escherichia coli, Biophys. J. 105 (2013) 172–181, https://doi.org/10.1016/j.bpj.2013.05.048.
[109] S. Bakshi, R.M. Dalrymple, W. Li, H. Choi, J.C. Weisshaar, Partitioning of RNA polymerase activity in live Escherichia coli from analysis of single-molecule diffusive trajectories, Biophys. J. 105 (2013) 2676–2686, https://doi.org/10.1016/j.bpj.2013.10.024.
[110] M. Stracy, C. Lesterlin, F. Garza de Leon, S. Uphoff, P. Zawadzki, A.N. Kapanidis, Live-cell superresolution microscopy reveals the organization of RNA polymerase in the bacterial nucleoid, PNAS. (2015), https://doi.org/10.1073/pnas.1507592112.
[111] J. Kim, A. Goni-Moreno, B. Calles, V. de Lorenzo, Spatial organization of the gene expression hardware in Pseudomonas putida, Env. Microbiol. (2019), https://doi.org/10.1111/1462-2920.14544.
[112] P. Montero Llopis, A.F. Jackson, O. Sliusarenko, I. Surovtsev, J. Heinritz, T. Emonet, C. Jacobs-Wagner, Spatial organization of the flow of genetic information in bacteria, Nature. 466 (2010) 77–81, https://doi.org/10.1038/nature09152.
[113] K. Nevo-Dinur, A. Nussbaum-Shochat, S. Ben-Yehuda, O. Amster-Choder, Translation-independent localization of mRNA in E. coli, Science. 331 (2011) 1081–1084, https://doi.org/10.1126/science.1195691.
[114] H. Bremer, P.P. Dennis, Modulation of chemical composition and other parameters of the cell at different exponential growth rates, EcoSal Plus 3 (2008) 1553–1569, https://doi.org/10.1128/ecosal.5.2.3.
[115] X. Weng, C.H. Bohrer, K. Bettridge, A.C. Lagda, C. Cagliero, D.J. Jin, J. Xiao, RNA polymerase organizes into distinct spatial clusters independent of ribosomal RNA transcription in E. coli, BioRxiv. (2018), 320481.
[116] Y.-W. Chang, S. Chen, E.I. Tocheva, A. Treuner-Lange, S. Löbach, L. Søgaard-Andersen, G.J. Jensen, Correlated cryogenic photoactivated localization microscopy and cryo-electron tomography, Nat. Methods 11 (2014) 737–739, https://doi.org/10.1038/nmeth.2961.
[117] D.M. van Elsland, S. Pujals, T. Bakkum, E. Bos, N. Oikonomeas-Koppasis, I. Berlin, J. Neefjes, A.H. Meijer, A.J. Koster, L. Albertazzi, S.I. van Kasteren, Ultrastructural imaging of Salmonella–host interactions using super-resolution correlative light-electron microscopy of bioorthogonal pathogens, ChemBioChem. 19 (2018) 1766–1770, https://doi.org/10.1002/cbic.201800230.
[118] L. Artzi, T. Dadosh, E. Milrot, S. Moraïs, S. Levin-Zaidman, E. Morag, E.A. Bayer, Colocalization and disposition of cellulosomes in Clostridium clariflavum as revealed by correlative superresolution imaging, MBio. 9 (2018) e00012–e00018, https://doi.org/10.1128/mBio.00012-18.
[119] M. Pohlschroder, S.V. Albers, Editorial: editorial for thematic issue on Archaea, FEMS Microbiol. Rev. 42 (2018) 719–720, https://doi.org/10.1093/femsre/fuy032.
[120] B. Turkowyd, D. Virant, U. Endesfelder, From single molecules to life: microscopy at the nanoscale, Anal. Bioanal. Chem. 408 (2016) 6885–6911, https://doi.org/10.1007/s00216-016-9781-8.
[121] S. Chimileski, M.J. Franklin, R.T. Papke, Biofilms formed by the archaeon Haloferax volcanii exhibit cellular differentiation and social motility, and facilitate horizontal gene transfer, BMC Biol. 12 (2014), 65, https://doi.org/10.1186/s12915-014-0065-5.
[122] I.G. Duggin, C.H. Aylett, J.C. Walsh, K.A. Michie, Q. Wang, L. Turnbull, E.M. Dawson, E.J. Harry, C.B. Whitchurch, L.A. Amos, J. Lowe, CetZ tubulin-like proteins control archaeal cell shape, Nature. 519 (2015) 362–365, https://doi.org/10.1038/nature13983.
[123] C.J. Reuter, J.A. Maupin-Furlow, Analysis of proteasome-dependent proteolysis in Haloferax volcanii cells, using short-lived green fluorescent proteins, Appl. Environ. Microbiol. 70 (2004) 7530–7538, https://doi.org/10.1128/AEM.70.12.7530-7538.2004.
[124] S. Maurer, K. Ludt, J. Soppa, Characterization of copy number control of two Haloferax volcanii replication origins using deletion mutants and haloarchaeal artificial chromo-

somes, J. Bacteriol. 200 (2018) e00517, https://doi.org/10.1128/JB.00517-17.
[125] T.D. Craggs, Green fluorescent protein: structure, folding and chromophore maturation, Chem. Soc. Rev. 38 (2009) 2865–2875, https://doi.org/10.1039/b903641p.
[126] A. Stoddard, V. Rolland, I see the light! Fluorescent proteins suitable for cell wall/apoplast targeting in Nicotiana benthamiana leaves, Plant Direct. 3 (2019), e00112, https://doi.org/10.1002/pld3.112.
[127] S. van de Linde, A. Loschberger, T. Klein, M. Heidbreder, S. Wolter, M. Heilemann, M. Sauer, Direct stochastic optical reconstruction microscopy with standard fluorescent probes, Nat. Protoc. 6 (2011) 991–1009, https://doi.org/10.1038/nprot.2011.336.
[128] T. Allers, S. Barak, S. Liddell, K. Wardell, M. Mevarech, Improved strains and plasmid vectors for conditional overexpression of His-tagged proteins in Haloferax volcanii, Appl Env. Microbiol. 76 (2010) 1759–1769, https://doi.org/10.1128/AEM.02670-09.
[129] V. Visone, W. Han, G. Perugino, G. Del Monaco, Q. She, M. Rossi, A. Valenti, M. Ciaramella, In vivo and in vitro protein imaging in thermophilic archaea by exploiting a novel protein tag, PLoS One 12 (2017), e0185791, https://doi.org/10.1371/journal.pone.0185791.
[130] T. Gristwood, I.G. Duggin, M. Wagner, S.V. Albers, S.D. Bell, The sub-cellular localization of Sulfolobus DNA replication, Nucleic Acids Res. 40 (2012) 5487–5496, https://doi.org/10.1093/nar/gks217.
[131] P.E. Schavemaker, W.M. Śmigiel, B. Poolman, Ribosome surface properties may impose limits on the nature of the cytoplasmic proteome, Elife. 6 (2017), e30084, https://doi.org/10.7554/eLife.30084.
[132] R. Zenke, S. von Gronau, H. Bolhuis, M. Gruska, F. Pfeiffer, D. Oesterhelt, Fluorescence microscopy visualization of halomucin, a secreted 927 kDa protein surrounding Haloquadratum walsbyi cells, Front. Microbiol. 6 (2015), 249, https://doi.org/10.3389/fmicb.2015.00249.
[133] R.Y. Samson, T. Obita, S.M. Freund, R.L. Williams, S.D. Bell, A role for the ESCRT system in cell division in archaea, Science. 322 (2008) 1710–1713, https://doi.org/10.1126/science.1165322.
[134] A.C. Lindas, E.A. Karlsson, M.T. Lindgren, T.J. Ettema, R. Bernander, A unique cell division machinery in the Archaea, Proc. Natl. Acad. Sci. U. S. A. 105 (2008) 18942–18946, https://doi.org/10.1073/pnas.0809467105.
[135] T.J. Ettema, A.C. Lindas, R. Bernander, An actin-based cytoskeleton in archaea, Mol. Microbiol. 80 (2011) 1052–1061, https://doi.org/10.1111/j.1365-2958.2011.07635.x.
[136] R. Wirth, A. Bellack, M. Bertl, Y. Bilek, T. Heimerl, B. Herzog, M. Leisner, A. Probst, R. Rachel, C. Sarbu, S. Schopf, G. Wanner, The mode of cell wall growth in selected archaea is similar to the general mode of cell wall growth in bacteria as revealed by fluorescent dye analysis, Appl. Environ. Microbiol. 77 (2011) 1556–1562, https://doi.org/10.1128/AEM.02423-10.
[137] A.W. Bisson-Filho, J. Zheng, E. Garner, Archaeal imaging: leading the hunt for new discoveries, Mol. Biol. Cell 29 (2018) 1675–1681, https://doi.org/10.1091/mbc.E17-10-0603.